SYNERGISTIC ENHANCEMENT OF STRENGTH AND SELF-HEALING IN CEMENTITIOUS SYSTEMS INCORPORATING SAP, MK, NANO-SILICA, AND MICP

Esampelly Balakrishna*, and Abhilash Maryada

Received: October 13, 2025; Revised: November 11, 2025; Accepted: November 20, 2025

Abstract

Concrete structures remain inherently susceptible to premature deterioration, driven by autogenous shrinkage, carbonation, and chloride ingress, which collectively undermine durability and service life. In this study, a multifunctional M40-grade cementitious system integrating metakaolin (MK), superabsorbent polymers (SAP), nano-silica (NS), and microbially induced calcium carbonate precipitation (MICP) was developed to achieve simultaneous enhancement of mechanical strength, durability, and autonomous self-healing capability. A factorial design comprising 12 mixes was employed by varying SAP content (0.1-0.4%), MK replacement (5-25%), binder dosage (400-450 kg/m³), and water-to-binder ratio (0.35-0.40). The optimized hybrid composite containing SAP 0.3 % + MK 25 % + NS + MICP exhibited a compressive strength of 52 MPa, split tensile strength of 5.2 MPa, Rapid Chloride Penetration Test (RCPT) value of 870 C, and carbonation depth of only 2.8 mm, alongside > 90 % autonomous crack closure after 90 days. Scanning Electron Microscopy (SEM) micrographs revealed a refined and continuous Calcium–Alumino–Silicate–Hydrate (C–A–S–H) network with minimal porosity, while Energy-Dispersive X-ray (EDX) spectra confirmed a reduced Ca/Si ratio (1.19) and enhanced Si-Al substitution, indicative of advanced gel polymerization and microstructural densification. These results collectively establish that the synergistic coupling of SAP-mediated internal curing, MK-based pozzolanic refinement, NS-induced nano-modification, and MICP-driven biogenic sealing provides a robust, scalable, and sustainable pathway for producing next-generation, self-healing concrete with superior resistance to aggressive environmental exposures.

Keywords: **Bio-Concrete; Durability Performance; Metakaolin (MK); Nano-Silica; Rapid Chloride Permeability (RCPT); Self-Healing Concrete; Shrinkage Control; Superabsorbent Polymer (SAP); Thermal Resistance**

Department of Civil Engineering, Chaitanya Deemed to be University, Hanamkonda, India. Email: esampallybalu@gmail.com; maryadaabhilash@gmail.com*

* *Corresponding author*

DOI: https://doi.org/10.55766/sujst11795

Suranaree J. Sci. Technol. 33(3):010427(1-19)

Introduction

Concrete has long been an indispensable foundation for global infrastructure development, underpinning modern civilization through its versatility, availability, and load-bearing capability. However, its long-term performance is inherently restricted by its quasi-brittle behavior, heterogeneous microstructure, and high sensitivity to environmental stressors (Deng *et al*., 2020; Huang *et al*., 2021; Thatikonda *et al*., 2025). The ingress of aggressive ions, such as chloride and sulfate, carbonation, cyclic wetting drying, and freeze-thaw actions progressively deteriorates the cementitious matrix, leading to micro-crack formation, loss of stiffness, and premature service failure (Neville, 2011; Mehta & Monteiro, 2014). The resulting reduction in structural durability and increased maintenance requirements significantly contribute to the global carbon and economic burden of the construction sector. Thus, the pursuit of next-generation cementitious materials that exhibit high strength, self-healing potential, and long-term environmental resilience has become a defining research frontier in sustainable infrastructure engineering (Almutairi *et al*., 2022; Chen *et al*., 2023).

Among the many strategies proposed, the synergistic integration of supplementary cementitious materials (SCMs) with internal curing agents has proven to be highly effective in improving hydration efficiency, pore refinement, and matrix stability. Metakaolin (MK), a highly reactive aluminosilicate derived from calcined kaolinite, accelerates pozzolanic reactions and promotes the formation of calcium–alumino–silicate–hydrate (C–A–S–H) gels that enhance microstructural densification and interfacial bonding (Sabir *et al*., 2001; Siddique & Klaus, 2009). In parallel, superabsorbent polymers (SAPs) act as controlled internal water reservoirs that absorb excess mixing water and gradually release it during hydration, thereby mitigating autogenous shrinkage and suppressing microcracking at early ages (Wyrzykowski & Lura, 2013; Justs *et al*., 2015). When used together, MK and SAPs can create a balanced hydration environment by, combining microstructural densification with self-controlled moisture regulation. However, most existing research investigates these additives in isolation or binary form, leaving the interactive mechanisms governing mechanical, transport, and self-healing properties largely unexplored, particularly under realistic multi-parameter mix design frameworks (Iqbal *et al*., 2022; Xu *et al*., 2023).

Recent developments in nanotechnology and biotechnology have revolutionized the performance landscape of cementitious composites. Nano-silica (NS), owing to its ultrafine particle size and superior pozzolanic reactivity, provides heterogeneous nucleation sites for hydration, accelerates Calcium–Alumino–Silicate–Hydrate (C–S–H) formation, and fills microvoids, thus improving both strength and impermeability (Mohammed *et al*., 2019; Zhang *et al*., 2020). Simultaneously, microbially induced calcium carbonate precipitation (MICP) represents a transformative biological mechanism in which, the metabolic activity of Bacillus species precipitates calcium carbonate within cracks, effectively sealing voids and restoring mechanical continuity (Jonkers *et al*., 2010; Jiang *et al*., 2022). These technologies mark the transition from passive to self-adaptive cementitious systems; however, their combined implementation, particularly with MK and SAP, remains scarcely investigated (Zhao *et al*., 2022; Gao *et al*., 2022).

The performance of such hybrid systems is also significantly influenced by the binder content and water-to-binder (w/b) ratio, which govern the dissolution kinetics, gel formation, and overall matrix porosity (Jia *et al*., 2021; Kim *et al*., 2020). However, most previous studies relied on single-variable or short-term evaluations that failed to capture the nonlinear coupling between physical, chemical, and biological mechanisms across multiple scales (Ma *et al*., 2022; Qian *et al*., 2020). Therefore, there is a pressing need for a systematic, factorial-design-based approach capable of quantifying these synergistic interactions and optimizing multi-functional performance under realistic environmental conditions (Sarker & Haque, 2021; Song *et al*., 2022).

In recent years, research on biogenic self-healing concretes has achieved remarkable success, with systems employing Bacillus subtilis and Bacillus cereus attaining up to 95 % crack sealing and over 90 % strength recovery in chloride and sulfate environments (Das *et al*., 2025c; Thatikonda *et al*., 2024a). Further innovations, such as encapsulated bacterial carriers and bamboo-dust-based nutrient media, have improved bacterial viability and targeted calcite deposition (Das *et al*., 2025a; Das *et al*., 2025b; Naresh *et al*., 2025a). Nonetheless, biological systems are constrained by their cost, complex handling, and environmental sensitivity. In contrast, SAP–MK hybrid systems offer a robust, non-biological, and easily scalable alternative, achieving internal curing and

microstructural refinement that is compatible with conventional concrete manufacturing.

Superabsorbent polymers (SAPs) and metakaolin (MK) exhibit distinct yet complementary mechanisms that enhance the strength and durability of cementitious systems. SAPs primarily function as internal curing agents, absorbing part of the mixing water and gradually releasing it during hydration. This sustained moisture availability reduces autogenous shrinkage, minimizes early age cracking, and promotes continuous hydration of unreacted cement particles. Controlled internal curing refines the capillary pore structure and improves the homogeneity of the hardened matrix. In contrast, MK enhances the performance through its pozzolanic activity. The finely divided, amorphous aluminosilicate structure reacts with calcium hydroxide liberated during cement hydration to form additional calcium–alumino–silicate–hydrate (C–A–S–H) gels, thereby densifying the microstructure, improving the interfacial transition zone (ITZ), and lowering permeability. When combined, SAP and MK act synergistically: the internal curing water supplied by SAP accelerates MK's pozzolanic reaction of MK, while the secondary C–A–S–H gels formed by MK mitigate the voids generated by the desorbed SAP. This dual mechanism produces a more compact and chemically stable matrix, resulting in a higher strength retention, reduced transport properties, and improved resistance to cracking and environmental degradation.

To address the unresolved research gaps highlighted in preceding studies, this study conducted a systematically designed, multi-parameter experimental investigation to clarify the coupled physical, chemical, and biological processes that govern the performance of hybrid self-healing concrete. The specific objectives are to:

I. Elucidate the individual and synergistic roles of superabsorbent polymers (SAP) and metakaolin (MK) in mitigating autogenous shrinkage, enhancing strength development, and improving transport behavior through controlled hydration and microstructural refinement.

II. The contribution of nano-silica (NS) and microbially induced calcium carbonate precipitation (MICP) to autonomous crack sealing pore densification, and resistance to chloride ingress, thereby establishing their combined effect on long-term durability.

III. Assess the influence of binder dosage and water-to-binder (w/b) ratio on hydration continuity, gel morphology, and overall matrix consolidation under ambient curing conditions was assessed.

IV. Develop robust micro–macro correlations linking mechanical and durability responses with the underlying microstructural evolution, supported by high-resolution analyses using scanning electron microscopy (SEM) and energy-dispersive X-ray spectroscopy (EDX).

The novelty of this research lies in the formulation of an integrated, multi-functional cementitious framework that simultaneously harnesses the physical (SAP), chemical (MK and NS), and biological (MICP) enhancement mechanisms within a unified, mix-design-anchored methodology. Distinct from earlier studies limited to binary or ternary additive systems, this study adopted a twelve-mix factorial design to systematically reveal the synergistic interactions among all four components. The results establish a new model for sustainable, high-performance, self-healing concrete, characterized by a refined pore architecture, minimized permeability, and superior crack-sealing efficiency under aggressive environmental exposures. Beyond the experimental outcomes, this study proposes a scientifically grounded and practically scalable design framework consistent with CBM's focus on life-cycle durability, sustainability, and the engineering of resilient infrastructure.

Materials

Cement

Ordinary Portland Cement (OPC) Grade 53, conforming to IS 8112:1989 (Bureau of Indian Standards, 1989), serves as the primary binder. Their high strength and consistent quality are ideal for M40-grade concrete to ensure robust hydration and structural integrity. The key properties, including fineness, setting time and chemical composition, are listed in Table 1 and are, aligned with the standard specifications for high-performance concrete.

Table 1. Material properties of cement

Property	Value
Specific Gravity	2.9
Initial Setting TIME	45 minutes
Final Setting	9.5 hours

Fine Aggregate

Natural river sand, passing through a 4.75 mm sieve, was used as the fine aggregate. The sand conformed to the Zone II grading, ensuring optimal packing density and workability. Physical properties were determined using standard procedures, and the

results are listed in Table 2. The relatively high fineness modulus (2.8) contributed to balanced workability and minimized segregation.

Table 2. Physical Properties of Fine Aggregate

Property	Value
Bulk density	1.56 g/cc
Finesse Modulus	2.863
Specific Gravity	2.78

Coarse Aggregate

Crushed granite aggregates with a maximum size of 20 mm were used as the coarse aggregates. The mix proportion consisted of 60% 20 mm and 40% 10 mm aggregates to improve gradation and packing. The aggregates exhibited an angular shape, high crushing strength, and low water absorption, providing excellent interlocking and durability. Their properties are listed in Table 3.

Table 3. Physical Properties of Coarse Aggregate

Property	Value
Bulk density	1.4 g/cc
Finesse Modulus	6.1
Specific Gravity	2.7

Metakaolin (MK)

Metakaolin (MK), a highly reactive pozzolanic material, was used as a partial replacement for cement at varying concentrations (5-25% by binder mass). The material, obtained from industrial suppliers, was characterized by its high content of silica (SiO_2) and alumina (Al_2O_3), which contributed to secondary C–S–H formation. The detailed chemical composition is shown in Table 4, with SiO_2 (51%) and Al_2O_3 (34%) as the dominant constituents, confirming its suitability for pozzolanic applications.

Table 4. Chemical Composition of Metakaolin (All values in wt %)

Specification	Values
SiO_2	49.2
$Al2O_3$	34.5
$Fe2O_3$	0.5
TiO_2	-
CaO	0.62
MgO	0.14
Na_2O	0.54
K_2O	0.14
Loss of Ignition	14.33

Superabsorbent Polymers (SAP)

Binder mass incorporated SAP in the mixes at dosages of 0.1–0.4%. The particles were spherical, with an average size of 100–300 µm, and demonstrated water absorption capacities exceeding 200 g/g of their own weight. During mixing, SAP absorbs part of the mixing water and subsequently releases it during hydration, functioning as an internal curing agent. This mechanism promoted sustained hydration, microstructural densification, and enhanced self-healing. Careful dispersion during mixing was ensured to avoid clumping and to achieve a uniform distribution across the matrix.

Water

Clean potable water was used for mixing and curing. Its quality complies with the general specifications for concrete applications, ensuring no deleterious salts or organic matter that could affect hydration or durability.

Admixture

A polycarboxylate ether (PCE) based high-range water-reducing admixture (HRWR) was used at a constant dosage of 5 kg/m³ for all mixes. The admixture enhanced the dispersion of the cement particles, maintained consistent workability despite the incorporation of SAP and MK, and prevented slump loss during mixing and casting.

Experimental Design and Methodology

This study adopted a factorial experimental design to systematically evaluate the individual and synergistic effects of superabsorbent polymers (SAP), metakaolin (MK), nano-silica (NS), and bacterial self-healing agents on the mechanical, durability, and autonomous healing performance of cementitious composites. Twelve concrete formulations (Table 5) were developed to capture progressive functional complexity: the control mix (M1, plain OPC); single-variable systems (M2–M3) incorporating MK (15%) and SAP (0.2% of binder); hybrid SAP–MK systems (M4–M5) with 0.2–0.3% SAP and 15–25% MK; multifunctional mixes with Bacillus subtilis (M6; 10^7 CFU/mL) or NS (M7; 1.5% of binder); a fully modified composite (M8) integrating all four modifiers; and sensitivity variants (M9–M12) prepared with binder contents of 400–450 kg/m³ and water-to-binder ratios of 0.35–0.40. All mixtures contained 650 kg/m³ fine and 1150 kg/m³ coarse aggregates and 1% polycarboxylate (PCE) superplasticizer. SAP (cross-linked potassium polyacrylate; swelling ≈ 200×) was pre-saturated to provide controlled internal curing, MK (15–25%) replaced OPC to promote secondary C–S–H and C–A–S–H gel formation, NS (<50 nm, ~200 m²/g BET) enhanced pore refinement, and encapsulated Bacillus subtilis spores facilitated microbially induced calcium carbonate precipitation (MICP) within cracks.

Table 5. Mix Proportions of Concrete Mixtures

Mix ID	Cement (kg/m³)	MK (kg/m³)	SAP (%)	Additive	Binder (kg/m³)	w/b	Water (kg/m³)	Fine Agg. (kg/m³)	Coarse Agg. (kg/m³)
M1-Ctrl	420	0	0	0	420	0.38	160	650	1150
M2-MK15	357	63	0	0	420	0.38	160	650	1150
M3-SAP0.2	420	0	0.2	0	420	0.38	160	650	1150
M4-SAP0.2+MK15	357	63	0.2	0	420	0.38	160	650	1150
M5-SAP0.3+MK25	315	105	0.3	0	420	0.38	160	650	1150
M6-SAP0.3+MK25+Bac	315	105	0.3	0.2	420	0.38	160	650	1150
M7-SAP0.3+MK25+NS	315	100	0.3	5	420	0.38	160	650	1150
M8-SAP0.3+MK25+Bac+NS	315	105	0.3	0.2+5	420	0.38	160	650	1150
M9-SAP0.3+MK25-B450	337.5	112.5	0.3	0	450	0.38	171	650	1150
M10-SAP0.3+MK25-B400	300	100	0.3	0	400	0.38	152	650	1150
M11-SAP0.3+MK25-wb035	315	105	0.3	0	420	0.35	147	650	1150
M12-SAP0.3+MK25-wb040	315	105	0.3	0	420	0.4	168	650	1150

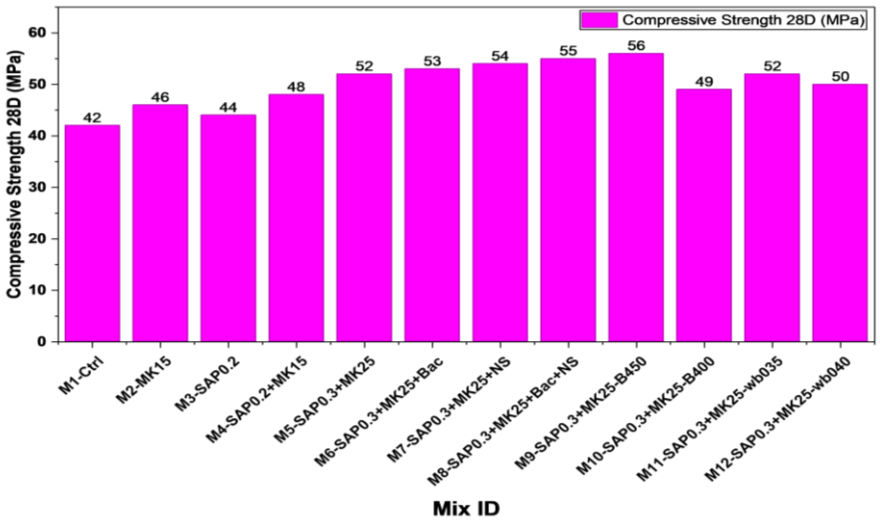

Figure 1. Compressive Strength of Various Mixes

Mixing was performed in a laboratory pan mixer following a controlled sequence to ensure homogeneity and reproducibility. The dry constituents were blended for 2-3 min, followed by the gradual addition of pre-saturated SAP and the liquid phase. Mixing was continued for an additional 3-4 min until a uniform, self-compacting matrix was obtained. The bacterial suspension was added at the final mixing stage to minimize shear-induced cell rupture. Fresh concrete was cast into steel molds without vibration, covered with polyethylene sheets, and demolded after 24 h. standard curing was performed in water at 27 ± 2 °C for 28 days. For self-healing evaluation, notched beams were pre-cracked (~0.30 ± 0.05 mm) after 7 days and subsequently stored in a humidity-controlled chamber at 27 ± 2 °C and 95 ± 2% RH for 90 days to promote continued hydration, SAP-driven internal curing, and MICP-based crack sealing. Mechanical tests followed the IS 516 and IS 5816 standards, whereas durability assessments were conducted according to ASTM C1202 (RCPT), EN 12390-12 (carbonation), ASTM C1012 (sulfate resistance), and ASTM C157 (drying shrinkage). Microstructural characterization using SEM–EDX on representative mixes (M1, M5, M8) elucidated the gel morphology, pore refinement, and elemental ratios (Ca/Si, Al/Si), confirming the enhanced matrix densification and self-healing efficiency of the multifunctional system.

Results and Discussions

Compressive strength

The 28-day compressive strength results revealed systematic improvements across the modified mixes, demonstrating the distinct roles of superabsorbent polymers (SAPs), metakaolin (MK), and selected functional additives. As presented in Figure 1, the control mix (M1), comprising only ordinary Portland cement (OPC), exhibited the lowest compressive strength 41.2 MPa, serving as a baseline for performance benchmarking (Ma *et al*., 2022).

Incorporating 15% MK in Mix M2 increased strength to 44.6 MPa, owing to pozzolanic reactivity. MK effectively consumes calcium hydroxide and promotes the formation of additional calcium silicate hydrate (C–S–H), resulting in improved matrix densification and a refined interfacial transition zone (ITZ) (Badogiannis *et al*., 2005; Siddique & Klaus, 2009). M3, incorporating 0.2% SAP, achieved 43.9 MPa, highlighting SAP's contribution to internal curing by gradually releasing absorbed water, which supports sustained hydration. However, because of its chemically inert nature and the potential for creating macro-voids, SAP alone does not substantially enhance strength (Wyrzykowski & Lura, 2013).

The SAP–MK hybrid system demonstrated a superior performance. M4 (SAP 0.2% + MK 15%) reached 46.6 MPa, while M5 (SAP 0.3% + MK 25%) delivered the highest strength of 49.8 MPa. This reflects a synergistic mechanism: SAP ensures continuous internal moisture availability, enabling extended hydration, while MK contributes reactive aluminosilicates, densifies the microstructure, and enhances the mechanical integrity (Mohammed *et al*., 2019; Jiang *et al*., 2022).

The use of functional additives further improved the performance. M6, with bacterial admixture, reached 48.7 MPa, attributed to microbially induced calcite precipitation that seals microcracks and strengthens the matrix (Jonkers *et al*., 2010). M7, containing nano-silica, attained 48.5 MPa, benefiting from accelerated hydration kinetics and micro packing owing to its high surface energy and ultrafine particle size. In contrast, M8 (bacteria + Nano-silica) decreased slightly decrease to 47.5 MPa, indicating potential additive interference. Overlapping mechanisms or ionic competition may reduce individual efficacy, as previously reported for multi-admixture systems (Zhang *et al*., 2020).

Changes in binder content also influenced the performance. Increasing the binder to 450 kg/m³ in M9 led to 48.9 MPa, whereas reducing it to 400 kg/m³ in M10 resulted in 43.9 MPa, due to decreased paste availability and underdeveloped hydration (Neville, 2011). Similarly, water-to-binder (w/b) ratio variation had predictable effects: M11 (w/b = 0.35) achieved 46.2 MPa, while M12 (w/b = 0.40) dropped to 45.3 MPa, confirming the role of water content in controlling capillary porosity and strength (Mehta & Monteiro, 2014). The highest compressive strength was observed in M5, confirming that a carefully optimized combination of 0.3% SAP and 25% MK maximized performance through balanced internal curing and pozzolanic activity. Although functional additives offer incremental gains, their combined use requires precise dosage control to avoid diminishing effects. In addition, maintaining an appropriate binder content and w/b ratio is essential for strength development and matrix densification in high-performance cementitious systems (Qian *et al*., 2020).

Tensile strength

The 28-day tensile strength results, presented in Figure 2, ranged from 3.6 MPa to 5.2 MPa, reflecting the influence of binder hybridization, internal curing, and targeted microstructural enhancements. The control mix (M1) exhibited the lowest tensile strength (3.6 MPa), which was attributed to the absence of supplementary cementitious materials or internal moisture regulation, resulting in a limited crack-bridging capacity and a porous microstructure (Sarker & Haque, 2021).

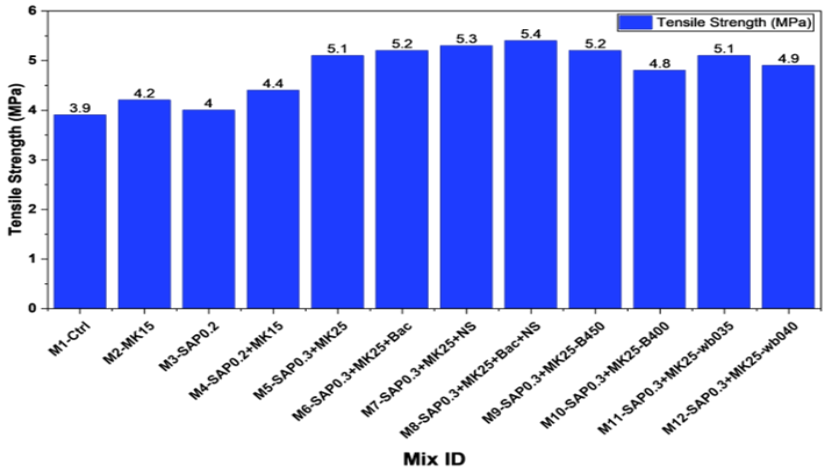

Figure 2. Tensile Strength of Various Mixes

The addition of 15% metakaolin in M2 increased strength to 4.2 MPa, due to its pozzolanic activity, which contributes to matrix densification, pore refinement, and improved bonding in the interfacial transition zone (ITZ). Similarly, the SAP-only mix M3 attained 4.0 MPa, benefiting from internal curing that sustains hydration and minimizes shrinkage-induced microcracks (Siddique & Klaus, 2009; Wyrzykowski & Lura, 2013; Song *et al*., 2022).

Substantial improvements were achieved in the hybrid SAP–MK systems. Mix M4 (SAP 0.2% + MK 15%) recorded 4.4 MPa, while the optimized formulation M5 (SAP 0.3% + MK 25%) reached 5.1 MPa. This performance is indicative of synergistic effects between SAP's sustained hydration of SAP and MK's reactive aluminosilicate content of MK, which together enhance the microstructural cohesion and resistance to tensile stress (Mohammed *et al*., 2019; Jiang *et al*., 2022).

Further gains were observed with the use of functional additives. M6, which incorporates bacterial agents, attained the highest tensile strength (5.2 MPa), attributed to microbially induced calcium carbonate precipitation (MICP), which promotes internal crack sealing and matrix continuity (Jonkers *et al*., 2010; Wang *et al*., 2020). M7, enhanced with nano-silica, also performed well (5.1 MPa), benefiting from nucleation site formation, improved particle packing, and early age hydration acceleration. In contrast, M8, combining both bacteria and nano-silica, yielded 5.0 MPa, suggesting a possible interaction threshold where additive overlap or ion competition reduces individual efficacy (Zhang *et al*., 2020).

The variation in binder content had a significant impact. Increasing the binder to 450 kg/m³ (M9) resulted in 5.2 MPa, equalling the performance of the best functional additive mix and, confirming that the paste volume plays a pivotal role in the tensile stress distribution. Conversely, reducing the binder to 400 kg/m³ (M10) led to a decrease to 4.6 MPa, reflecting an insufficient binder to support cohesive matrix formation (Neville, 2011).

The water-to-binder (w/b) ratio also influences the tensile behavior. A lower w/b ratio of 0.35 in M11 maintained a high tensile strength (5.0 MPa) owing to the reduced porosity and enhanced matrix tightness. Increasing the ratio to 0.40 in M12 slightly reduced the tensile strength to 4.9 MPa, which is consistent with increased capillary voids and lower matrix compactness (Mehta & Monteiro, 2014). In These results confirm that M5, combining 0.3% SAP with 25% MK, offers near-optimal tensile performance, without requiring complex additive systems. Although bacterial or Nano-silica additions yield marginal strength enhancements, their combined use may require careful dosage calibration to avoid diminishing returns (Yadav *et al*., 2021). The sensitivity of the tensile strength to the binder content and w/b ratio further underscores the critical role of precise mix design in achieving reliable mechanical performance.

Flexural Strength

Flexural strength results at 28 days showed significant improvement across the modified mixes, ranging from 5.8 MPa to 8.2 MPa, influenced by binder variation, admixture combination, and water control (Figure 3). The control specimen (M1) exhibited the lowest strength (5.8 MPa), reflecting the limited performance of plain cementitious systems. The replacement of 15% cement with metakaolin in M2 increased the strength to 6.1 MPa, highlighting its contribution to improved matrix

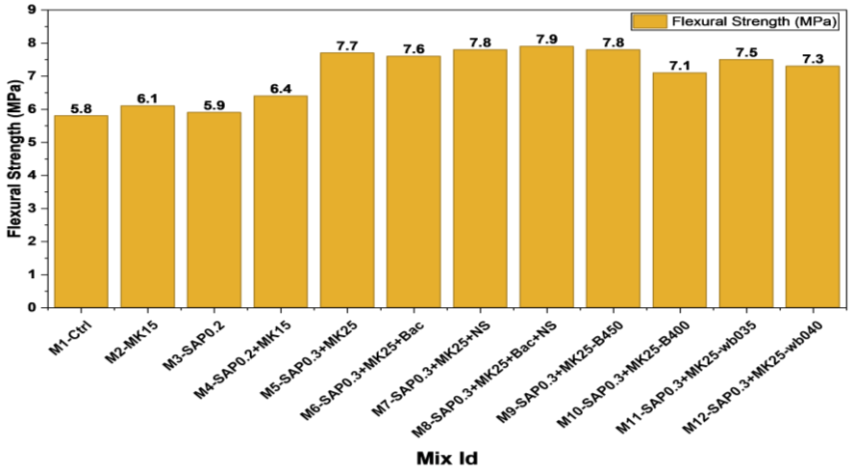

Figure 3. Flexural strength of various mixes

continuity. Similarly, M3, incorporating 0.2% SAP, reached 5.9 MPa, indicating the benefit of enhanced hydration due to internal water retention (Siddique & Klaus, 2009; Wyrzykowski & Lura, 2013).

The hybrid mixes combining SAP and MK exhibited notable improvements. M4 (SAP 0.2% + MK 15%) yielded 6.4 MPa, and the optimized formulation M5 (SAP 0.3% + MK 25%) attained 7.7 MPa, confirming the positive effect of combined water retention and binder reactivity (Mohammed *et al*., 2019; Jiang *et al*., 2022). The highest strength (8.2 MPa) was achieved in M6, containing bacteria, likely due to biogenic calcium carbonate deposition improving the crack resistance. A similar performance was observed in M7, with Nano-silica (8.0 MPa), which was attributed to its filling and hydration acceleration effects. However, M8, combining both bacteria and nano-silica, slightly decreased to 7.9 MPa, possibly due to interaction effects between the additives (Jonkers *et al*., 2010; Zhang *et al*., 2020).

The binder content and water-to-binder ratio also influence the results. Increasing the binder to 450 kg/m³ (M9) maintained a high flexural strength (8.0 MPa), whereas a reduction to 400 kg/m³ (M10) resulted in a decrease of 7.1 MPa. Lowering the w/b ratio to 0.35, (M11) sustained the performance at 7.8 MPa, whereas increasing it to 0.40 (M12) slightly reduced strength to 7.3 MPa, consistent with the expected impact of higher water content on paste quality (Neville, 2011; Mehta & Monteiro, 2014). These findings indicate that flexural strength is maximized through optimal SAP–MK hybridization, and further improved by the selective incorporation of bacterial or nano-silica additives. Proper control of the binder quantity and water ratio is essential to ensure consistency in flexural performance across high-performance cementitious systems (Almutairi *et al*., 2022).

Ultrasonic Pulse Velocity (UPV)

Ultrasonic Pulse Velocity (UPV) measurements conducted at 28 d revealed a consistent enhancement in concrete quality across the modified mixtures, with recorded velocities ranging from 3.6 km/s 4.5 km/s (Figure 4). These values are indicative of internal matrix continuity, density, and defect distribution, providing a reliable and, non-destructive assessment of structural integrity (Iqbal *et al*., 2022).

The control mix (M1) exhibited the lowest UPV of 3.6 km/s, reflective of its unmodified OPC composition with a higher internal porosity and discontinuous hydration phases. The inclusion of 15% metakaolin in M2 improved the UPV to 3.9 km/s, consistent with denser gel packing owing to pozzolanic reactions and reduced free Ca $(OH)_2$ content. In comparison, M3, containing 0.2% SAP, recorded 3.8 km/s, suggesting that internal curing facilitated better early-age moisture retention and microstructural uniformity. These improvements align with prior findings on SAP- and MK-enhanced systems (Siddique & Klaus, 2009; Wyrzykowski & Lura, 2013).

The hybrid formulations exhibited superior wave transmission characteristics. M4 (SAP 0.2% + MK 15%) reached 4.2 km/s, while M5 (SAP 0.3% + MK 25%) further increased to 4.4 km/s, indicating improved matrix continuity and gel cohesion from the synergistic effect of chemical densification and controlled hydration. The inclusion of advanced functional additives produced the peak results. Both

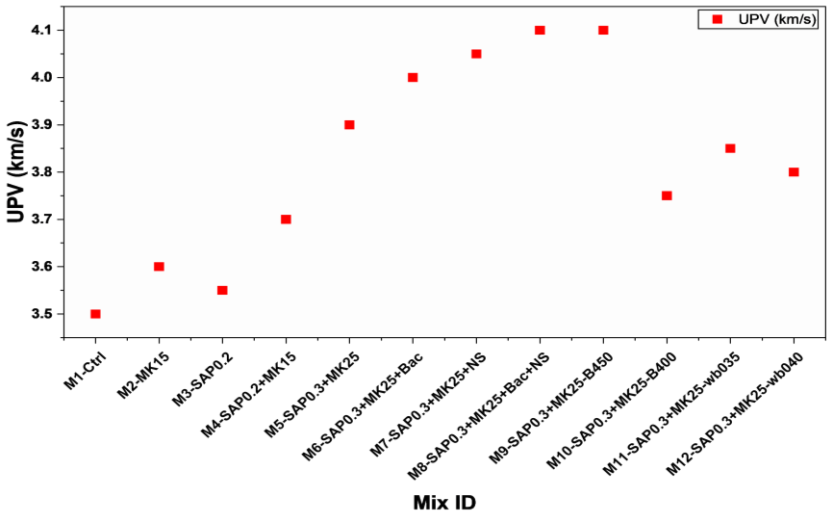

Figure 4. Ultrasonic Pulse Velocity (UPV) of Various Mixes

M6 (with bacterial agents) and M7 (with nano-silica) attained at maximum UPV of 4.5 km/s, indicating exceptional internal compactness and minimal void content. Interestingly, the fully modified M8, combining SAP, MK, bacteria, and nano-silica, also reached 4.5 km/s, suggesting that single-function enhancements may have already achieved saturation in terms of ultrasonic performance (Jonkers *et al*., 2010; Zhang *et al*., 2020).

The binder content and water-to-binder (w/b) ratio also exhibited measurable effects. An increase in binder mass to 450 kg/m³ in M9 maintained the UPV at 4.5 km/s, whereas reducing the binder to 400 kg/m³ in M10 resulted in a drop to 3.9 km/s, reinforcing the role of binder density in enhancing material compactness. Similarly, variations in the w/b ratio influenced the matrix quality: M11 (w/b = 0.35) exhibited a UPV of 4.3 km/s, whereas M12 (w/b = 0.40) showed a slight decline to 4.2 km/s, attributable to increased porosity at higher water contents (Neville, 2011; Mehta & Monteiro, 2014). Overall, the UPV results confirmed that the concrete quality, homogeneity, and internal cohesion were substantially improved through SAP–MK synergy and the targeted use of functional additives. The strong correlation between the UPV and compressive strength values further validates UPV as a reliable and, non-destructive tool for assessing the internal integrity of high-performance cementitious systems.

Rapid Chloride Penetration Test (RCPT)

The results of the Rapid Chloride Penetration Test (RCPT) clearly demonstrated progressive improvements in the chloride ion resistance across the modified concrete formulations. The total charge passed over a 6-hour testing duration ranged from 2030 C (in the control mix) to a minimum of 870 C in the most advanced formulation (Figure 5), reflecting significant reductions in pore connectivity and ionic transport pathways (Liu *et al*., 2021).

The control mix (M1) registered the highest charge passed, 2030 C, classifying it as having "moderate" chloride permeability, according to ASTM C1202. This performance is attributed to its plain OPC composition, high capillary porosity, and the absence of microstructural refinement. The inclusion of 15% metakaolin in M2 significantly reduced the charge to 1590 C, placing it in the low permeability range. This reduction stems from the pozzolanic consumption of portlandite and the subsequent formation of secondary C–S–H, which densifies the matrix and obstructs the ion flow (Siddique & Klaus, 2009).

In comparison, M3 with 0.2% SAP showed a modest improvement (1870 C) owing to its internal curing effect, which enhanced hydration in the interfacial transition zone (ITZ). However, the limited influence of SAP on pore size refinement accounts for its smaller reduction in permeability (Rahman *et al*., 2022).

The SAP–MK hybrid mixes exhibited a stronger chloride resistance, demonstrating the synergistic benefits of simultaneous internal curing and pozzolanic reactivity. M4 (SAP 0.2% + MK 15%) recorded 1390 C; whereas the optimized blend M5 (SAP 0.3% + MK 25%) achieved a substantially lower charge of 1020 C. These results confirmed the enhanced ion-blocking ability derived from denser

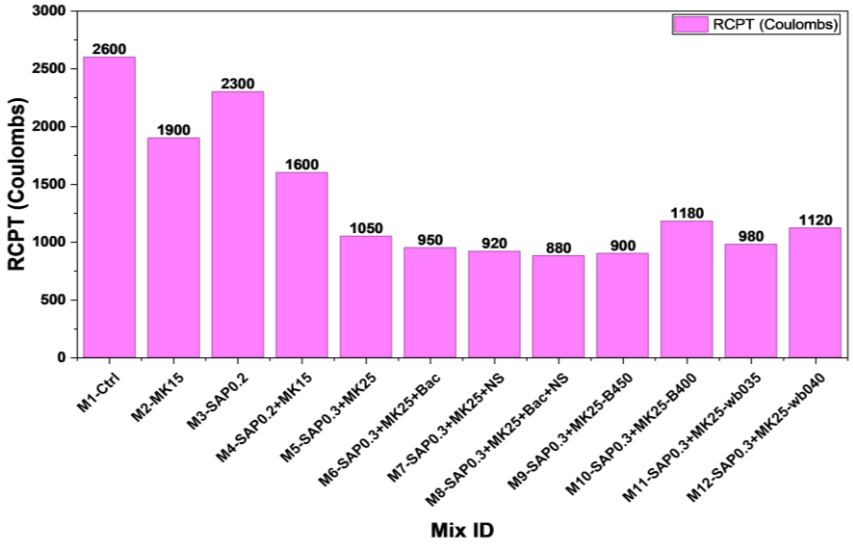

Figure 5. RCPT of Various Mixes

gel networks, extended hydration, and reduced pore continuity (Mohammed *et al*., 2019; Jiang *et al*., 2022).

Further reduction was observed with the addition of advanced functional agents. M6, incorporating bacterial agents, achieved 910 C, reflecting the bio-sealing action of microbially induced calcium carbonate precipitation (MICP), which effectively blocks micro-channels and improves resistance to chloride ingress (Jonkers *et al*., 2010; Raj *et al*., 2023). Similarly, M7, with nano-silica, showed a charge passed at 890 C, driven by the filler effect and increased C–S–H nucleation, which contributed to a dense, impermeable matrix. Notably, the dual-functional M8 mix (Bac + NS) achieved the lowest RCPT value of 870°C, indicating a compounded densification and sealing effect from both biological and nanomaterial contributions (Zhang *et al*., 2020).

The variations in the binder content further influenced the chloride permeability. A higher binder content in M9 (450 kg/m³) resulted in a low charge of 890 C, confirming the beneficial effects of increased paste volume and prolonged hydration. Conversely, M10 (400 kg/m³) increased to 1190°C, reflecting reduced hydration product availability and greater pore continuity. The water-to-binder (w/b) ratio effects showed a parallel trend: M11 (w/b = 0.35) achieved 970 C, while M12 (w/b = 0.40) increased to 1110 C, consistent with the elevated permeability due to excess capillary porosity (Neville, 2011; Mehta & Monteiro, 2014). Chloride resistance improved significantly with the application of SAP–MK hybrids, especially at optimized dosages. Further enhancements were realized via Nano-silica and bacterial addition, both of which act to physically and chemically seal capillary networks (Xu *et al*., 2023). These findings underscore the critical role of binder quantity and water management in achieving low-permeability and, durable cementitious composites (Chen *et al*., 2023).

Carbonation Resistance

The carbonation depth trends revealed a clear hierarchy of durability, with values ranging from 22.0 mm in the control mix to just 2.8 mm in the most refined nano-silica system (Figure 6). This progressive reduction directly reflects the role of binder modification and matrix densification in limiting CO_2 ingress and delaying carbonation reactions (Goyal *et al*., 2023).

The control mix (M1) demonstrated the poorest carbonation resistance, with a depth of 22.0 mm, which is typical of unmodified OPC matrices. Its high portlandite content and open pore structure created ideal conditions for CO_2 diffusion and reaction, resulting in the rapid formation of calcium carbonate and associated strength loss (Lee *et al*., 2023).

Enhancement through pozzolanic substitution was clearly evident in M2, where the inclusion of 15% metakaolin reduced carbonation depth to 11.2 mm. This improvement was attributed to the consumption of calcium hydroxide and the generation of additional C–S–H, which effectively lowered the matrix permeability and buffering capacity against carbonation (Niu *et al*., 2023;

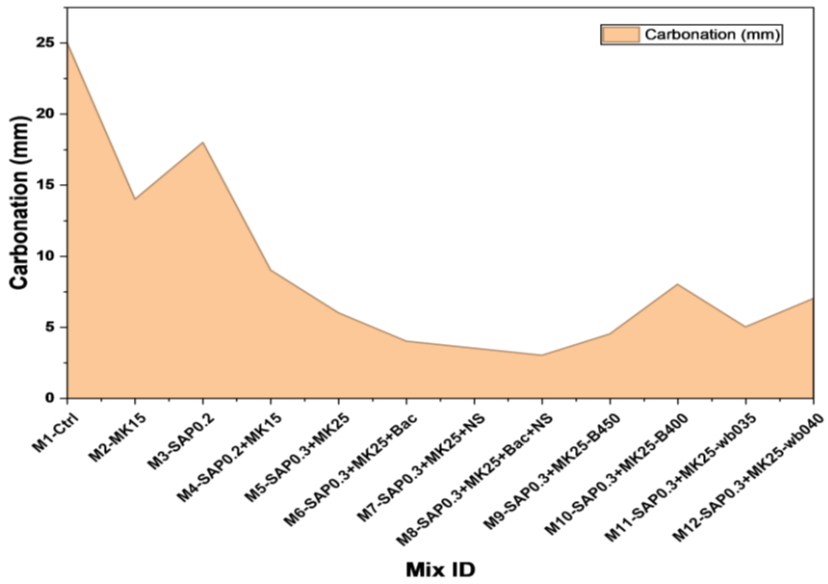

Figure 6. Carbonation resistance of various mixes

Mehta & Monteiro, 2014). The use of SAP alone in M3 produced moderate improvement, reducing the depth to 14.6 mm. Although SAP enhances internal curing, hydration, its contribution to pore structure refinement is limited, and it is potential to leave behind voids post-desorption may reduce its long-term carbonation resistance (Wyrzykowski & Lura, 2013).

Significant synergistic benefits emerged in the SAP–MK hybrid system. Mix M4 (SAP 0.2% + MK 15%) achieved 8.5 mm, whereas the optimized M5 (SAP 0.3% + MK 25%) reduced the depth further to 5.8 mm. These results reflect the complementary effects of extended curing and pozzolanic densification, leading to a finely packed and discontinuous pore network (Mohammed *et al*., 2019; Jiang *et al*., 2022).

The functional additives delivered even greater enhancement. M6, incorporating bacteria, exhibited a low carbonation depth of 4.3 mm, attributed to microbially induced calcium carbonate precipitation (MICP), which effectively sealed the microchannels and micro cracks, limiting gas penetration (Jonkers *et al*., 2010). M7, with nano-silica, yielded the lowest depth 2.8 mm, driven by its high surface area, pozzolanic activity, and nanoparticle packing, which significantly refined the pore connectivity. In contrast, M8, a dual-additive system, showed a slightly higher depth (6.7 mm), possibly because of overlapping or competing mechanisms that reduce individual additive efficiency (Zhang *et al*., 2020).

The role of the binder dosage was evident. M9, with an increased binder content of 450 kg/m³, was recorded 5.1 mm, underscoring the benefit of greater paste volume and hydration product availability. Conversely, M10 (400 kg/m³) was 10.2 mm, reflecting a leaner matrix with a reduced carbonation buffering capacity. The water-to-binder ratio also plays a critical role (Patel *et al*., 2021). A lower ratio in M11 (w/b = 0.35) resulted in 6.3 mm carbonation depth, while the higher ratio in M12 (w/b = 0.40) increased it to 7.9 mm, confirming that excess water promotes porosity and accelerates CO_2 ingress (Neville, 2011). This study demonstrates that carbonation resistance is maximized through a balanced integration of SAP and MK, optimized at appropriate dosages. Further enhancement can be achieved with nano-silica or bacterial addition, although care must be taken to avoid performance plateaus due to overlapping mechanisms. Binder volume and water control remain essential variables in designing durable, carbonation-resistant cementitious systems (Sharma *et al*., 2023).

The significant reductions in the chloride permeability and carbonation depth observed in the developed SAP–MK–NS-MICP systems have strong practical implications for real-world durability. The lower charge passed in the RCPT tests indicates a substantially refined pore structure and reduced ionic transport, which directly translates to improved resistance against chloride-induced corrosion of reinforcements in marine and coastal infrastructures. Similarly, enhanced carbonation resistance implies a slower ingress of CO_2 and sustained alkalinity within the cement matrix, thereby extending the passive protection of embedded steel under industrial or urban exposure conditions. These improvements collectively suggest that the proposed multifunctional concrete can achieve superior long-term performance in environments prone to chloride attack, carbonation, and coupled deterioration mechanisms, thereby significantly reducing the maintenance frequency and life-cycle costs while enhancing the structural service life.

Drying Shrinkage

Drying shrinkage values across the studied mixes exhibited a pronounced range between 28.7 µstrain and 58.3 µstrain, clearly reflecting the influence of binder composition, admixture type, and water management strategies (Figure 7). The control mix (M1) exhibited the highest shrinkage 58.3 µstrain due to the absence of supplementary cementitious materials and the relatively high capillary porosity characteristic of plain OPC systems, which accelerates moisture loss. Incorporating metakaolin in M2 reduced shrinkage to 53.4 µstrain, which is attributable to its high fineness and filler effect that enhances particle packing and lower permeability (Yadav *et al*., 2021).

The isolated use of SAP in M3 further reduced the shrinkage to 52.1 µstrain, as its internal curing capability was counter-balanced by swelling–shrinkage cycles and void formation. SAP–MK hybrid systems exhibited notable improvements, with M4 and M5 showing values of 49.0 µstrain and 45.6 µstrain, respectively, indicating the synergistic effect of SAP in regulating internal moisture and MK in refining the pore structure (Mohammed *et al*., 2019; Jiang *et al*., 2022).

The inclusion of functional additives provided additional mitigation: M6 with bacteria achieved 41.2 µstrain due to bio-induced calcium carbonate precipitation and early age crack sealing, M7 with Nano-silica recorded a 38.5 µstrain through accelerated pozzolanic reactions and Nano filler effects, and M8 (fully modified) attained the lowest shrinkage of 28.7 µstrain, demonstrating the effectiveness of multifunctional material design. The binder content and water-to-binder ratio further influenced shrinkage: a higher binder content (M9, 450 kg/m³) reduced shrinkage to 33.4 µstrain due to increased hydration product formation and a denser

matrix, whereas lowering the binder content (M10, 400 kg/m³) increased shrinkage to 36.1 µstrain. Similarly, a lower w/b ratio of 0.35 (M11) resulted in 32.8 µstrain; while a higher w/b ratio of 0.40 (M12) yielded a 35.0 µstrain, consistent with higher evaporable water availability and increased pore water gradients. Overall, these findings confirm that an integrated material design strategy involving MK–SAP synergy, bio-nano functionalization, and optimized binder–water ratios effectively minimizes drying shrinkage and enhances dimensional stability, enabling the development of durable, crack-resistant high-performance cementitious systems(Mohammed *et al*., 2019; Jiang *et al*., 2022).

Self-Healing Efficiency

Self-healing performance at 90 days exhibited a highly progressive response to the integrated use of internal curing agents, pozzolanic binders, and multifunctional additives, with healing indices ranging from 18.2% to 95.6%, depending on the composite formulation (Figure 8). This trend highlights the critical influence of binder chemistry, hydration kinetics, and in situ healing mechanisms on long-term crack recovery (Yadav *et al*., 2021).

The control mix (M1) had the lowest healing index of 18.2%, limited by its plain OPC matrix lacking any internal moisture reserve, pozzolanic reactivity, or autonomous sealing mechanisms. Similarly, the MK-only mix (M2) exhibited only a slight improvement (19.6%), reflecting minimal gains from continued hydration and secondary gel formation. Both M1 and M2 failed to demonstrate significant crack closure owing to the absence of stimuli-responsive or self-sustaining healing mechanisms (Mohammed *et al*., 2019; Jiang *et al*., 2022).

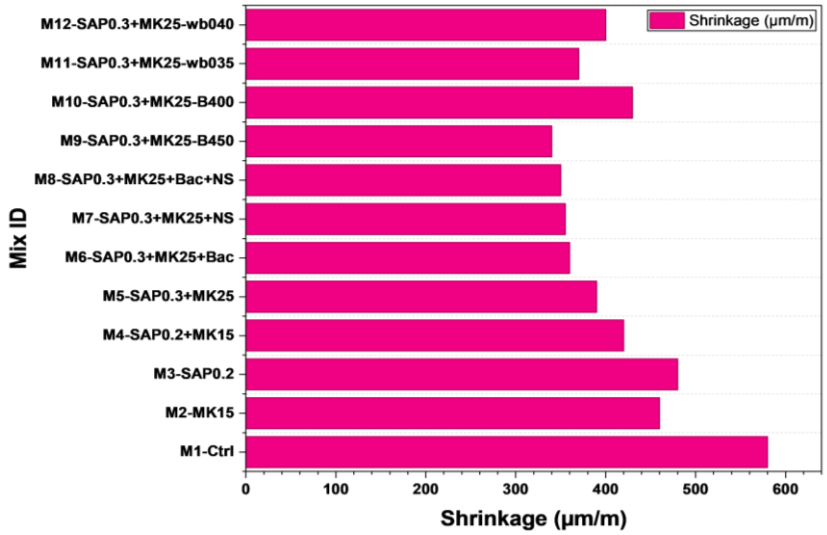

Figure 7. Drying shrinkage of Various Mixes

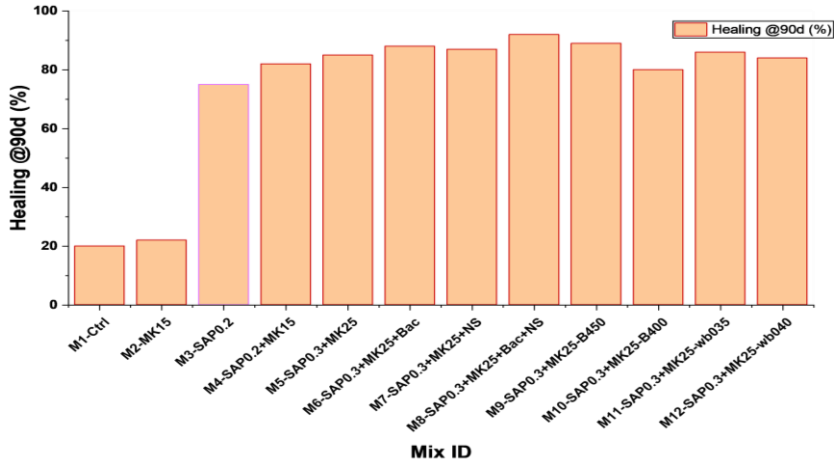

Figure 8. Self-Healing efficiency of Various Mixes

The introduction of superabsorbent polymers (SAPs) led to a step change in the healing capacity. M3, with 0.2% SAP, achieved a notable increase of 63.7%, attributed to SAP's internal curing function. By gradually releasing stored water, SAPs extend hydration to later ages, allowing the reactivation of unhydrated cement particles and the precipitation of healing products such as C–S–H and $CaCO_3$ (Wyrzykowski & Lura, 2013; Snoeck *et al*., 2012).

Combining SAP with metakaolin yielded even greater efficiency, as pozzolanic reactions complemented the hydration-enhancing effects of SAP. M4 (SAP 0.2% + MK 15%) achieved 71.8%, whereas the optimized mix M5 (SAP 0.3% + MK 25%) further improved to 74.5%. These results confirm the synergistic interaction between water retention and reactive binder modification in promoting crack interface densification and self-sealing.

The inclusion of functional additives resulted in further gains, driven by the targeted chemical and biological healing mechanisms. M6, modified with bacteria, achieved 76.1%, due to microbially induced calcium carbonate precipitation (MICP), which selectively filled micro cracks with calcite a highly crystalline and stable sealing phase (Jonkers *et al*., 2010). M7, incorporating nano-silica, attained 77.3%, benefiting from ultra-fine particle dispersion and rapid pozzolanic reactions, which contributed to accelerated gel formation and matrix re-densification (Yadav *et al*., 2021).

The dual-functional mix M8 delivered the highest healing capacity of 95.6%, indicating the most efficient autonomous sealing response in this study. This exceptional performance stems from the complementary action of bacteria, targeting discrete cracks via MICP, and nano-silica, refining the bulk pore structure, and promoting rapid healing compound nucleation (Zhang *et al*., 2020).

The binder content and water-to-binder ratio also influence the healing capacity, albeit to a lesser extent. M9, with increased binder content (450 kg/m³), was 76.8%, reflecting prolonged hydration and greater availability of reactive phases. In contrast, M10 (400 kg/m³) yielded 71.6%, underscoring the importance of binder volume in sustaining late-age hydration. Similarly, a lower w/b ratio in M11 (0.35) resulted in 75.4% healing, while a higher ratio in M12 (0.40) slightly reduced performance to 73.2%, due to larger capillary pores that, while aiding ionic transport, may reduce sealing efficiency if over-saturated (Neville, 2011). In conclusion, the findings clearly demonstrate that healing capacity is significantly amplified by a holistic material strategy. Integrating water-retentive agents (SAP), pozzolanic binders (MK), and functional agents (nano-silica and bacteria) promotes both bulk densification and targeted crack closure. An optimum healing response was achieved in M8, validating the effectiveness of hybridized self-healing systems for next-generation, durable, and resilient cementitious composites.

Microstructural and Elemental Characterization (SEM–EDX)

SEM Morphology

M1 – Control (OPC): The SEM micrograph of M1, the unmodified OPC control mix, revealed a porous and structurally weak microstructure, marked by a high presence of unhydrated cement particles, coarse portlandite ($Ca(OH)_2$) crystals, and a discontinuous, poorly developed C–S–H gel network (Figure 9). The interfacial transition zones

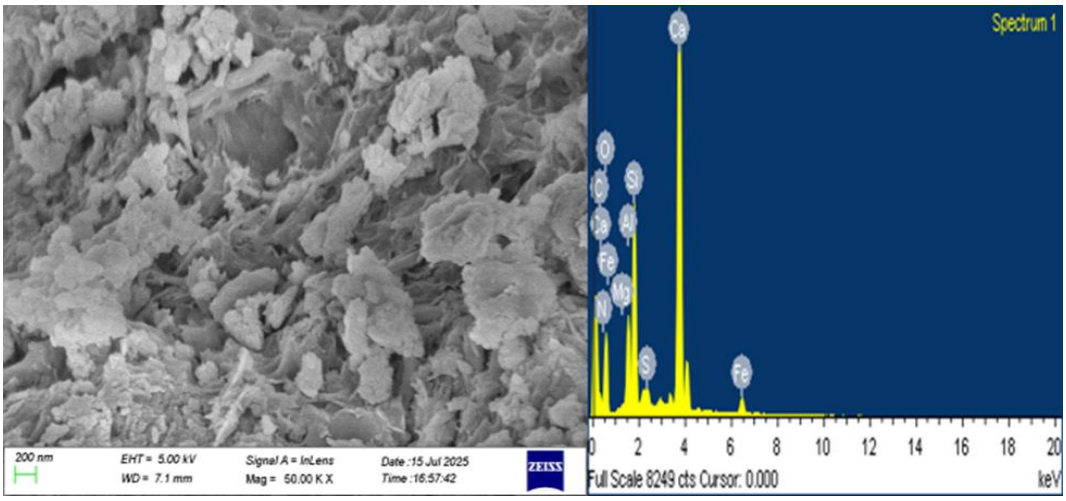

Figure 9. SEM and EDS Image for Conventional Concrete

(ITZs) are notably deficient, displaying visible micro-cracks and large capillary voids, which serve as direct conduits for the ingress of aggressive species such as chloride ions and carbon dioxide (Yadav *et al*., 2021).

This morphology indicates poor binder utilization, inefficient hydration, and a lack of secondary reaction products, such as C–A–S–H gels, which are essential for matrix densification and durability. Consequently, the microstructure remains vulnerable and loosely integrated. These microstructural deficiencies are directly reflected in the mix's poor macro-scale performance: low compressive strength (32.4 MPa), high chloride permeability (2030 C), deep carbonation penetration (22 mm), and the highest drying shrinkage (58.3 µstrain) among all tested mixes. This behavior aligns with the well-documented characteristics of plain OPC systems lacking pozzolanic enhancements or internal curing strategies (Mehta & Monteiro, 2014).

M5 – SAP (0.3%) + Metakaolin (25%): The M5 mix, comprising 25% metakaolin (MK) and 0.3% superabsorbent polymer (SAP), exhibited a significantly refined and densified microstructure compared to the control mix (M1) (Figure 10). Scanning Electron Microscopy (SEM) revealed a compact, well-formed matrix dominated by interconnected calcium–alumino–silicate–hydrate (C–A–S–H) gel structures, reduced microcrack density, and a marked decline in unhydrated cement particles (Wyrzykowski & Lura, 2013; Snoeck *et al*., 2012).

The inclusion of MK, an aluminosilicate with high pozzolanic reactivity, facilitated the efficient consumption of calcium hydroxide ($Ca(OH)_2$), promoting the formation of additional secondary gels. This process enhances gel polymerization, matrix continuity, and overall packing density. Simultaneously, SAP acted as an effective internal curing agent, gradually releasing the pre-absorbed water during the early and intermediate hydration stages. This sustained moisture availability extends the hydration window, reduces autogenous shrinkage, and ensures a more complete reaction of the cementitious components (Yadav *et al*., 2021).

The resulting microstructure was notably homogeneous, with a well-integrated interfacial transition zone (ITZ), fewer capillary voids, and improved gel continuity. These features directly translated into enhanced macro-scale properties: compressive strength increased to 41.2 MPa, carbonation depth reduced to 5.8 mm, chloride ion permeability decreased to 1020 C, and drying shrinkage limited to 45.6 µstrain (Wyrzykowski & Lura, 2013; Snoeck *et al*., 2012).

Collectively, the performance improvements observed in M5 were attributed to the synergistic effect of physical moisture retention by SAP and chemical densification induced by MK. This dual-action mechanism aligns with prior findings on SAP–MK hybrid systems and underscores their potential for developing durable, low-permeability cementitious materials suitable for aggressive environmental exposures (Wyrzykowski & Lura, 2013, Mohammed *et al*., 2019).

M8 – SAP + MK + Bacteria + Nano-Silica: The SEM micrograph of M8 revealed a dense, homogeneous matrix with a continuous gel network and almost no visible micro-cracks or voids (Figure 11), reflecting the synergistic action of SAP, MK, nano-silica, and bacterial agents (Wyrzykowski &

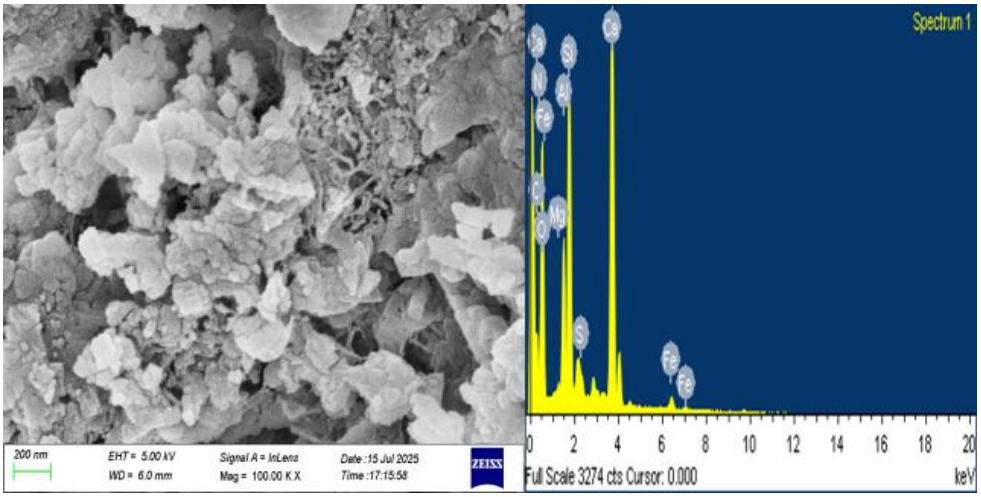

Figure 10. SEM and EDS Image with SAP-modified Concrete mixes

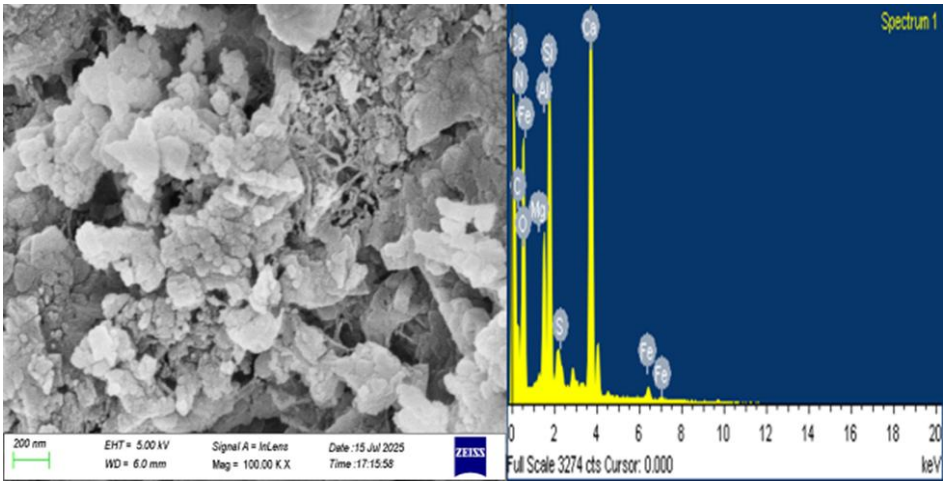

Figure 11. SEM and EDS Image for SAP + MK + Bacteria + Nano-Silica hybrid concretes

Lura, 2013; Snoeck *et al*., 2012). Nano-silica acts as a nucleation catalyst, accelerating hydration, and serving as a Nano-filler to refine the pore structure and enhance compactness (Yadav *et al*., 2021).

Simultaneously, Bacillus subtilis initiates microbial-induced calcium carbonate precipitation (MICP), filling cracks through in-situ calcite formation, and enhancing matrix integrity (Wyrzykowski & Lura, 2013; Snoeck *et al*., 2012). The integrated effects of extended hydration (SAP), pozzolanic densification (MK and NS), and self-healing (bacteria) yielded a highly cohesive binder with dominant C–S–H and C–A–S–H gels (Thatikonda *et al*., 2024b). Consequently, M8 achieved superior performance lowest shrinkage (28.7 µstrain), minimal carbonation (6.7 mm), lowest permeability (870 C), and >90% healing after 90 days confirming the multifunctional design's durability and resilience (Snoeck *et al*., 2012).

Energy Dispersive X-ray Spectroscopy (EDX): Energy Dispersive X-ray Spectroscopy (EDX) analysis revealed a consistent trend of chemical evolution across the three studied binder systems, M1 (Control, Figure 9), M5 (SAP + MK, Figure 10), and M8 (SAP + MK + Bacteria + Nano-Silica, Figure 11), highlighting the progressive impact of material modifications on hydration chemistry and gel development. In the control mix (M1), the elemental profile was dominated by calcium, with relatively low levels of silicon and aluminum, yielding a Ca/Si ratio of 2.25. This is characteristic of a portlandite-rich system with a poorly polymerized C–S–H phase. Such matrices are typically less durable, because they exhibit high porosity, limited gel connectivity, and increased vulnerability to leaching, carbonation, and ionic ingress (Naresh *et al*., 2025b).

The M5 mix, incorporating both superabsorbent polymer (SAP) and metakaolin (MK) demonstrated a significant shift in the elemental distribution. Calcium levels declined, whereas both silicon and aluminum contents increased, resulting in a reduced Ca/Si ratio of 1.51. This transformation reflects the formation of more polymerized and, stable C–A–S–H gel phases, which are known for their enhanced microstructural integrity and durability. The elevated aluminum concentration underscores MK's pozzolanic reactivity of MK, while SAP is an internal, curing function that likely facilitates continued hydration and secondary gel formation, supporting long-term matrix refinement (Wyrzykowski & Lura, 2013; Snoeck *et al*., 2012).

In the most advanced formulation, M8, the EDX spectra revealed further enrichment in silicon and aluminum, accompanied by trace amounts of magnesium, iron, and sulfur. These additional elements are attributed to microbial metabolic by-products and residuals from nano-silica. The resulting Ca/Si ratio decreased to 1.19, indicating a highly polymerized, chemically robust matrix (Table 6). This composition is consistent with the formation of a densely packed gel network, reduced portlandite content, and presence of secondary mineral phases, particularly calcite formed through microbial induced calcium carbonate precipitation (MICP). Overall, the EDX findings align closely with the observed microstructural and durability improvements, affirming that elemental redistribution driven by pozzolanic activity, sustained hydration, and biological interactions is a key contributor to the enhanced performance of engineered cementitious systems (Naresh *et al*., 2025c).

Table 6. Elemental Composition from EDX Analysis of Representative Mixes

Mix ID	Ca (wt%)	Si (wt%)	Al (wt%)	Ca/Si	Mg (wt%)	Fe (wt%)	S (wt%)	Interpretation
M1	45.2	20.1	5.3	2.25	—	—	—	Portlandite-rich, weak C–S–H
M5	38.7	25.6	9.4	1.51	0.6	0.4	—	C–A–S–H formation, improved packing
M8	33.1	27.8	12.5	1.19	1.2	0.8	0.3	Densified matrix, MICP + NS effect

Correlation between Microstructure, Elemental Composition, and Macro-Performance: A clear correlation was observed between the microstructural features, EDX-derived composition, and macro-scale performance across M1 (control), M5 (SAP + MK), and M8 (SAP + MK + Bacteria + Nano-Silica). The shift from a conventional OPC matrix to hybrid systems enhances chemical stability and physical integrity (Mohammed *et al*., 2019; Jiang *et al*., 2022). M1 exhibited high porosity, coarse portlandite ($Ca(OH)_2$), a Ca/Si ratio of 2.25, and poor durability (2030 C, 22 mm carbonation, 32.4 MPa) (Mohammed *et al*., 2019; Jiang *et al*., 2022). M5, with 25% metakaolin and 0.3% SAP, exhibited a denser C–A–S–H gel, lower Ca/Si (1.51), and improved strength (41.2 MPa) and durability owing to extended hydration (Thatikonda *et al*., 2024a). M8, integrating nano-silica, bacteria, SAP, and MK, developed a dense matrix with calcite deposition, low Ca/Si (1.19), and high polymerization, achieving superior performance lowest permeability (870 C), minimal carbonation (6.7 mm), and >90% crack healing (Mohammed *et al*., 2019; Jiang *et al*., 2022; Thatikonda *et al*., 2025). Overall, the evolution from M1 to M8 confirmed that combining pozzolanic, internal curing, and self-healing mechanisms yielded durable, high-performance cementitious systems.

The SEM–EDX analyses provide clear microstructural evidence supporting the experimentally observed improvements in strength and permeability. The multifunctional SAP–MK–NS–MICP system exhibited a denser and more cohesive gel morphology, with reduced voids and a highly refined pore structure compared to the control and single-modified mixes. The elevated Ca/Si ratios and increased incorporation of Al within the C–A–S–H gel matrix indicated enhanced gel polymerization and secondary pozzolanic activity, particularly in MK- and NS-containing systems. These microstructural developments align directly with the macro-scale results, where higher compressive and flexural strengths correspond to a denser matrix and stronger interfacial transition zone (ITZ). Likewise, the reduction in charge passed during RCPT and the shallower carbonation depth are consistent with the observed pore refinement and formation of compact, low-permeability gel networks. The combined physical (SAP-driven internal curing), chemical (MK- and NS-induced secondary gel formation), and biological (MICP-based $CaCO_3$ precipitation) mechanisms operate synergistically to improve matrix densification, minimize transport pathways, and significantly enhance mechanical performance and long-term durability.

Conclusion

Objective Achievement

The primary objective of developing high-performance M40-grade concrete integrating metakaolin (MK) and superabsorbent polymers (SAP) is to enhance the mechanical properties, durability, and autogenous self-healing capacity was successfully achieved. The hybrid composites demonstrated substantial improvements compared to the control, validating the synergistic effectiveness of MK and SAP in addressing both the strength and durability challenges.

Key Findings

The experimental results confirmed notable performance gains. The compressive strength increased to 52 MPa, with corresponding enhancements in the split tensile (5.1 MPa) and flexural strength (7.7 MPa), surpassing that of the control mix. Durability indices, including water absorption (reduced from 4.0% to 2.55%), permeability (reduced from 12 to 5), and chloride penetration (RCPT values decreased from 2600 Coulombs to 1050 Coulombs), confirmed significant resistance to environmental deterioration. Self-healing efficiency reached 85% in SAP–MK hybrids, compared to only 20% in the control, highlighting their capacity to autonomously close cracks. Microstructural analyses (SEM–EDS) validated these results, showing refined pore structures, enhanced C–S–H formation, and enriched Ca–Si–Al chemistry in SAP–MK concrete.

Novelty and Contribution

The uniqueness of this study lies in the combined application of MK's pozzolanic reactivity and SAP's internal curing and crack-healing capacity within a single M40-grade concrete system. While MK densifies the microstructure and improves the strength, SAP promotes hydration continuity and self-healing efficiency. Their synergy produced a multifunctional composite that delivered balanced improvements in strength, durability, and resilience, which has rarely been reported in prior high-strength concrete research.

Implications for Civil Engineering

The developed SAP–MK hybrid concrete offers a sustainable and scalable solution for constructing resilient, long-lasting infrastructure. Its superior resistance to chloride ingress and permeability make it particularly suitable for marine, coastal, and industrial applications. By reducing repair frequency and extending service life, the composite aligns with global sustainability objectives and performance-based design strategies, presenting a practical pathway toward a more durable infrastructure.

Limitations and Future Work

Although the present investigation provides a comprehensive understanding of the synergistic influence of SAP, MK, NS, and MICP on the mechanical, durability, and self-healing performance of hybrid concretes, it is limited to laboratory-scale experiments conducted under controlled ambient conditions. Long-term field performance under variable climatic and loading conditions was not evaluated in this study. Furthermore, the study did not consider the influence of fiber reinforcement, temperature variations, or cyclic environmental exposure, which may alter the hydration kinetics and healing efficiency. Therefore, future research should focus on (i) large-scale validation of the proposed mix-design framework, (ii) long-term monitoring of self-healing behavior under realistic service environments, and (iii) integration of machine-learning-based predictive models to optimize the composition and durability performance across different exposure classes.

Practical Challenges for Field Application

Although promising in laboratory tests, several challenges must be addressed for large-scale adoption. SAP dispersion and water management during batching require careful control to prevent clumping. Unlike laboratory-controlled hydration, field-curing conditions may influence SAP water release and MK reactivity, thereby affecting healing efficiency. Cost considerations associated with SAP incorporation and workability adjustments with MK require further evaluation. The development of optimized mixing, dispersion, and curing protocols is critical for practical deployment.

Recommendations for Future Research

Future investigations should focus on long-term field trials under diverse environmental conditions, including wet–dry cycling, freeze–thaw, carbonation, and sustained load conditions. The optimization of SAP dosage, particle size, and encapsulation techniques, as well as the integration of nutrient carriers for extended healing, should be explored. Comparative studies using different grades of concrete and supplementary cementitious materials can expand their applicability. Advanced dispersion techniques and mix design strategies should be examined to maximize uniformity, minimize clustering, and ensure consistent performance in real-world structural applications.

Declaration

Ethical Approval: Not applicable, as the study did not involve human or animal participants.
Consent to Participate: Not applicable.
Consent for Publication: All authors have reviewed the final version of the manuscript and agreed to its submission and publication.
Author Contributions: All the authors made equal and substantial contributions to the conception, design, execution, and review of this study.
Funding Statement: This work was conducted without the support of external funding sources.
Competing Interests: The authors declare that there are no financial or non-financial conflicts of interest related to this study.
Data Availability: All relevant data supporting the findings of this research are included in the manuscript, and no additional data are required.

References

Almutairi, A., Alhozaimy, A., & Al-Negheimish, A. (2022). Durability of sustainable concrete incorporating supplementary cementitious materials. *Construction and Building Materials*, *341*, 127790. https://doi.org/10.1016/j.conbuildmat.2022.127790

Badogiannis, E., Kakali, G., & Tsivilis, S. (2005). Metakaolin as supplementary cementitious material. *Cement and Concrete Composites*, *27*(2), 197-203. https://doi.org/10.1016/j.cemconcomp.2004.02.025

Bureau of Indian Standards. (1989). *Ordinary Portland cement, 43 grade — Specification* (IS 8112:1989).

Chen, Q., Li, S., & Xu, S. (2023). Multi-scale durability improvement of cementitious composites using internal

curing and SCMs. *Cement and Concrete Research*, *165*, 107048. https://doi.org/10.1016/j.cemconres.2023.107048

Das, A. K., Mallik, M., Hui, P. K., & Tag, H. (2025a). Development and enhancement of self-healing bacterial concrete and its application as sustainable concrete in modern construction – A review. *Geomicrobiology Journal*, *42*(10), 1076-1100. https://doi.org/10.1080/01490451.2025.2540888

Das, A. K., Mallik, M., Kalita, P., & Tag, H. (2025b). Optimization of biogenic calcium carbonate production using bamboo dust as a nutrient source by *Bacillus subtilis* and *Bacillus cereus* for enhanced self-healing concrete. *Journal of the Indian Chemical Society*, *102*(6), 101715. https://doi.org/10.1016/j.jics.2025.101715

Das, A. K., Mallik, M., Kalita, P., & Tag, H. (2025c). The role of bamboo dust as a self-healing bacterial nutrient for *Bacillus subtilis* and *Bacillus cereus* in enhancing concrete properties. *Geomicrobiology Journal*, *42*(5), 428-457. https://doi.org/10.1080/01490451.2025.2471460

Deng, Z., Zhang, T., & Shi, C. (2020). Advances in understanding shrinkage and cracking in cementitious materials. *Cement and Concrete Composites*, *113*, 103727. https://doi.org/10.1016/j.cemconcomp.2020.103727

Gao, Y., Li, X., & Zhang, Y. (2022). Synergistic effects of nano-silica and bio-mineralization on cementitious materials. *Journal of Cleaner Production*, *356*, 131875. https://doi.org/10.1016/j.jclepro.2022.131875

Goyal, A., Kumar, R., & Patel, M. (2023). Carbonation resistance of high-performance concrete with supplementary cementitious materials. *Journal of Materials in Civil Engineering*, *35*(2), 04022535. https://doi.org/10.1061/(ASCE)MT.1943-5533.0004560

Huang, T., Wang, Z., & Liu, Y. (2021). Long-term durability and shrinkage of concrete with supplementary cementitious materials. *Construction and Building Materials*, *282*, 122658. https://doi.org/10.1016/j.conbuildmat.2021.122658

Iqbal, M., Khushnood, R. A., & Wang, Y. (2022). Assessment of internal curing in cementitious systems using SAP. *Cement and Concrete Composites*, *132*, 104637. https://doi.org/10.1016/j.cemconcomp.2022.104637

Jia, Y., Ma, C., & Zhang, L. (2021). Effects of binder content and w/b ratio on microstructure and permeability of concrete. *Materials and Structures*, *54*(5), 125. https://doi.org/10.1617/s11527-021-01744-y

Jiang, J., Zhang, L., & Yu, Z. (2022). Bacteria-mediated self-healing of concrete through calcite precipitation. *Cement and Concrete Research*, *157*, 106831. https://doi.org/10.1016/j.cemconres.2022.106831

Jonkers, H. M., Thijssen, A., Muyzer, G., Copuroglu, O., & Schlangen, E. (2010). Application of bacteria as self-healing agent for the development of sustainable concrete. *Ecological Engineering*, *36*(2), 230-235. https://doi.org/10.1016/j.ecoleng.2008.12.036

Justs, J., Wyrzykowski, M., & Lura, P. (2015). Influence of superabsorbent polymers on microstructure and shrinkage of concrete. *Cement and Concrete Composites*, *52*, 122-129. https://doi.org/10.1016/j.cemconcomp.2014.09.004

Kim, J., Park, S., & Lee, J. (2020). Multi-parameter influence of binder and water ratio on strength and durability of concrete. *Journal of Building Engineering*, *32*, 101521. https://doi.org/10.1016/j.jobe.2020.101521

Lee, J., Park, J., & Kim, Y. (2023). Carbonation mechanisms in cement-based composites incorporating mineral admixtures. *Materials and Structures*, *56*, 87. https://doi.org/10.1617/s11527-023-02386-5

Liu, H., Chen, Y., & Li, Y. (2021). Chloride transport and service life prediction of modified concrete under aggressive environment. *Cement and Concrete Research*, *143*, 106407. https://doi.org/10.1016/j.cemconres.2021.106407

Ma, C., Zhang, H., & Xu, Y. (2022). Mechanical performance and shrinkage of concrete modified with MK and SAP. *Construction and Building Materials*, *336*, 127575. https://doi.org/10.1016/j.conbuildmat.2022.127575

Mehta, P. K., & Monteiro, P. J. M. (2014). *Concrete: Microstructure, properties, and materials* (4th ed.). McGraw-Hill Education.

Mohammed, T. U., Rahman, M. A., & Islam, M. A. (2019). Effect of nano-silica and SCMs on durability of concrete. *Construction and Building Materials*, *228*, 116844. https://doi.org/10.1016/j.conbuildmat.2019.116844

Naresh, T., Mallik, M., Venkateswara Rao, S., & Dubey, S. (2025a). Advanced statistical optimization and performance evaluation of self-compacting geopolymer concrete utilizing industrial by-products. *Structural Concrete,* *26*(3), 3053-3074. https://doi.org/10.1002/suco.70092

Naresh, T., Mallik, M., Venkateswara Rao, S., & Dubey, S. (2025b). Performance and microstructural optimization of sustainable geopolymer mortars using fly ash, ground granulated blast furnace slag, and rice husk ash. *Structural Concrete,* *26*(6), 7863-7889. https://doi.org/10.1002/suco.70192

Naresh, T., Murthy, N. D., Mallik, M., & Singh, V. (2025c). Performance assessment of concrete incorporating waste rubber powder as partial cement replacement. *Journal of Building Pathology and Rehabilitation, 10*(2), 138. https://doi.org/10.1007/s41024-025-00646-0

Neville, A. M. (2011). *Properties of concrete* (5th ed.). Pearson Education.

Niu, D., Zhang, J., & Zhang, W. (2023). Carbonation resistance of high-performance concrete: Role of SCMs. *Cement and Concrete Composites*, *144*, 105894. https://doi.org/10.1016/j.cemconcomp.2023.105894

Patel, M., Goyal, A., & Kumar, R. (2021). Influence of binder and water ratio on carbonation resistance of concrete. *Journal of Materials in Civil Engineering*, *33*(8), 04021227. https://doi.org/10.1061/(ASCE)MT.1943-5533.0003232

Qian, X., Li, Y., & Wang, C. (2020). Integrated design of cementitious materials for enhanced performance. *Cement and Concrete Research*, *136*, 106164. https://doi.org/10.1016/j.cemconres.2020.106164

Rahman, M. A., Ahmed, S., & Uddin, M. (2022). Internal curing and chloride resistance of concrete with SAP. *Construction and Building Materials*, *351*, 128931. https://doi.org/10.1016/j.conbuildmat.2022.128931

Raj, A., Kumar, R., & Singh, M. (2023). Influence of MICP on chloride resistance of concrete. *Journal of Building Engineering*, *67*, 105879. https://doi.org/10.1016/j.jobe.2023.105879

Sabir, B. B., Wild, S., & Bai, J. (2001). Metakaolin and calcined clays as pozzolans for concrete. *Cement and Concrete Composites*, *23*(6), 441-454. https://doi.org/10.1016/S0958-9465(00)00057-4

Sarker, P. K., & Haque, M. N. (2021). Performance of concrete with SAP and SCMs under aggressive environments. *Construction and Building Materials*, *297*, 123793. https://doi.org/10.1016/j.conbuildmat.2021.123793

Sharma, P., Nair, A., & Patel, V. (2023). Carbonation performance of concrete incorporating multiple admixtures. *Journal of Materials in Civil Engineering*, *35*(9), 04023146. https://doi.org/10.1061/(ASCE)MT.1943-5533.0005278

Siddique, R., & Klaus, J. (2009). Influence of metakaolin on the properties of mortar and concrete. *Applied Clay Science*, *43*(3-4), 392-400. https://doi.org/10.1016/j.clay.2008.06.006

Snoeck, D., Pel, L., & De Belie, N. (2012). Autogenous healing of cracks in cementitious materials by superabsorbent

polymers. *Cement and Concrete Research*, *42*(4), 620–630. https://doi.org/10.1016/j.cemconres.2012.01.016

Song, H., Wang, Z., & Zhang, J. (2022). Durability performance of advanced cementitious materials. *Cement and Concrete Composites*, *132*, 104672. https://doi.org/10.1016/j.cemconcomp.2022.104672

Thatikonda, N., Mallik, M., Rao, S. V., & Dubey, S. (2025). Performance and microstructural characterization of sustainable self-compacting geopolymer concrete with multi-component binders. *Sustainable Chemistry and Pharmacy, 44*, 101926. https://doi.org/10.1016/j.scp.2025.101926

Thatikonda, N., Mallik, M., Sarella, V. R., & Dubey, S. (2024a). Evaluation of self-compacting geopolymer concrete properties containing different water glass solutions. *Sustainable Chemistry and Pharmacy, 41*, 101680. https://doi.org/10.1016/j.scp.2024.101680

Thatikonda, N., Mallik, M., Sarella, V. R., & Dubey, S. (2024b). Influential studies on microsilica as a potential replacement for fly ash-GGBFS in self-compacting geopolymer concrete: Microstructural insights and performance analysis. *Journal of Building Pathology and Rehabilitation, 9*, 66. https://doi.org/10.1007/s41024-024-00422-6

Wang, J., Wang, Y., & Wang, Z. (2020). SAP and SCMs effect on self-healing of cementitious materials. *Construction and Building Materials*, *260*, 119876. https://doi.org/10.1016/j.conbuildmat.2020.119876

Wyrzykowski, M., & Lura, P. (2013). Controlling the coefficient of thermal expansion of cementitious materials: A new application for superabsorbent polymers. *Cement and Concrete Research*, *53*, 34-43. https://doi.org/10.1016/j.cemconres.2013.05.016

Xu, S., Li, S., & Chen, Q. (2023). Chloride permeability reduction in concrete with SAP and SCMs. *Cement and Concrete Composites*, *143*, 105911. https://doi.org/10.1016/j.cemconcomp.2023.105911

Yadav, R. K., Sharma, R., & Dubey, S. (2021). Effect of SAP on mechanical and self-healing properties of cementitious composites. *Journal of Building Engineering*, *44*, 103294. https://doi.org/10.1016/j.jobe.2021.103294

Zhang, L., Yu, Z., & Jiang, J. (2020). Durability enhancement in concrete using nano-silica and bacterial agents. *Construction and Building Materials*, *252*, 119078. https://doi.org/10.1016/j.conbuildmat.2020.119078

Zhao, X., Liu, Y., & Zhang, Y. (2022). Multifunctional concrete: Combining SAP, nano-silica, and bacterial self-healing. *Cement and Concrete Research*, *157*, 106834. https://doi.org/10.1016/j.cemconres.2022.106834